Self-Assembled Electrical Biodetector Based on Reduced Graphene Oxide
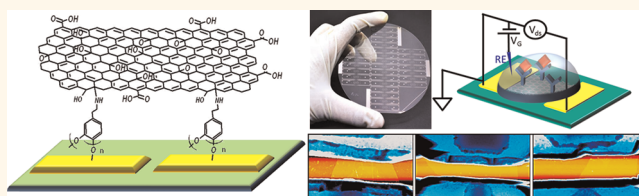
Tetiana Kurkina,[†,*] Subramanian Sundaram,[†,⊥] Ravi Shankar Sundaram,[†,#] Francesca Re,[‡] Massimo Masserini,[‡] Klaus Kern,[†,§] and Kannan Balasubramanian[†,*]

[†]Max Planck Institute for Solid State Research, Heisenbergstrasse 1, D-70569 Stuttgart, Germany, [‡]Dipartimento di Medicina Sperimentale, Università degli Studi di Milano-Bicocca, Via Cadore 48, I-20052 Monza, Italy, and [§]Institut de Physique de la Matière Condensée, Ecole Polytechnique Fédérale de Lausanne, CH-1015 Lausanne, Switzerland. [⊥]Present address: Department of Electrical Engineering and Computer Science, Massachusetts Institute of Technology, Cambridge, MA 02139, USA. [#]Present address: Center for Advanced Photonics and Electronics (CAPE), Engineering Department, University of Cambridge, 9, JJ Thomson Avenue, Cambridge, CB3 0FA, UK. The manuscript was written through contributions of all authors. All authors have given approval to the final version of the manuscript.

The electronic and mechanical properties of graphene and its derivatives make it an attractive material for the development of devices with applications in various fields, such as field-effect transistors, capacitors, and mass, optical, or electrical sensors.[1−7] However it is still challenging to obtain such devices in a routine and scalable manner. Mechanical exfoliation of graphene from a graphite crystal followed by electron beam lithography is the commonly used technique for the preparation of contacted graphene flakes.[8] This approach is widely used in research laboratories, but has a number of limitations that make it unsuitable for device production at an industrial level because of the critical manual operation steps that cannot be automated. Moreover the geometry of the flakes and the layout of the contacts vary from one chip to another. This can complicate manufacturing processes and the operation of the devices at later stages. Researchers are trying to overcome these limitations by using CVD (chemical vapor deposition)-grown graphene as a starting material for device fabrication.[9−11] Alternatively, solution-based fabrication approaches have been tested, offering promise for large-scale processing without the use of bulky equipment or very high temperatures. In such cases, a graphene suspension is obtained from graphite through intercalation of graphitic layers using organic solvents or surfactants.[12−14] The disadvantages of this approach include the low yield, the small sizes of the flakes, and the inhomogeneity of the suspensions, attributed mainly to the highly hydrophobic character of graphene.[15,16]

A strategy to overcome the hydrophobicity aspect involves the preparation of an aqueous solution of an oxidized form of graphene, namely, graphene oxide (GO).[17] Due to the presence of polar groups such as hydroxyl, carboxyl, and epoxy groups,[18] GO is very hydrophilic in comparison to graphene. For the purpose of device applications, the drawback when using GO is that it is an insulating material. This can be overcome by the use of a reduction procedure, which improves its conductivity,[17] yielding reduced graphene oxide (RGO). Fabrication of RGO devices has been demonstrated by drop casting an aqueous solution, followed by search and contacting.[19] Alternatively, ac dielectrophoresis can be used to trap the flakes at predefined locations.[20−22]

ABSTRACT

Large-scale fabrication of graphene-based devices is an aspect of great importance for various applications including chemical and biological sensing. Toward this goal, we present here a novel chemical route for the site-specific realization of devices based on reduced graphene oxide (RGO). Electrodes patterned by photolithography are modified with amino functional groups through electrodeposition. The amine groups function as hooks for the attachment of graphene oxide flakes selectively onto the electrodes. Graphene-like electrical behavior is attained by a subsequent thermal annealing step. We show that this anchoring strategy can be scaled-up to obtain RGO devices at a wafer scale in a facile manner. The scalability of our approach coupled with the use of photolithography is promising for the rapid realization of graphene-based devices. We demonstrate one possible application of the fabricated RGO devices as electrical biosensors through the immunodetection of amyloid beta peptide.

KEYWORDS: graphene · reduced graphene oxide · chemical functionalization · biosensors · amyloid beta

However, the scalability of such approaches is very limited due to the need to address every device individually during the fabrication process.

Here we report a chemical route for the realization of devices starting from GO. Our strategy utilizes the presence of reactive oxygen-containing functional groups on the surface of GO. The procedure involves the electrochemical rendering of photolithographically patterned electrodes with amino groups. These amino groups react with the functional groups on the GO surface, leading to the immobilization of the GO flakes selectively at the electrode locations. Electrode gaps of around 4 μm could be easily bridged using this procedure. The fixed GO flakes are subsequently reduced by a thermal annealing process to obtain RGO, showing graphene-like field-effect behavior. Furthermore, we demonstrate that this procedure can be scaled-up to obtain RGO devices on 4 in. glass wafers with low resistances and a high device yield of more than 80%. The obtained RGO-FET devices in liquid-gated configuration can be used as electrical biosensors. For this purpose we have realized an RGO-based immunosensor for the detection of amyloid beta (Aβ) peptide, the peptide that is commonly associated with Alzheimer's disease.[23]

RESULTS AND DISCUSSION

The protocol behind the chemical anchoring procedure is outlined in Figure 1. Individual Si/SiO$_2$ substrates prewritten with electrodes (45 nm Ti/8 nm Pt) incorporating a gap (4 μm) are utilized to demonstrate the principle. In the first step, the platinum electrodes were modified by oxidative electropolymerization (see Experimental Section) of tyramine (Figure 1a), leading to the formation of a thin polytyramine film (pTy). The film has a high density of free amino groups (Figure 1b),[24] and its height can be controlled by the parameters of electrochemical functionalization.[25] Subsequently, the pTy-functionalized chips are incubated in a GO solution (see Supporting Information) for one hour at room temperature, during which the GO flakes are immobilized selectively on the electrode surface (Figure 1c). It has been reported that the epoxy groups on the GO surface are responsible for a good coupling to the amine groups.[26] The coupling mechanism is also supported by previous studies demonstrating the immobilization of biomolecules on tyramine-functionalized microelectrodes.[27,28] Finally, the samples are annealed in argon at 350 °C for 60 min. This serves two purposes, namely, the removal of the pTy film and simultaneously the reduction of oxygen-containing groups to a large extent (Figure 1d).

The substrate surface was characterized using atomic force microscopy (AFM) at various stages of the anchoring protocol. Figure 2a presents a final AFM image of the sample (at the end of the protocol) along with line profiles (Figure 2b) from AFM images taken at
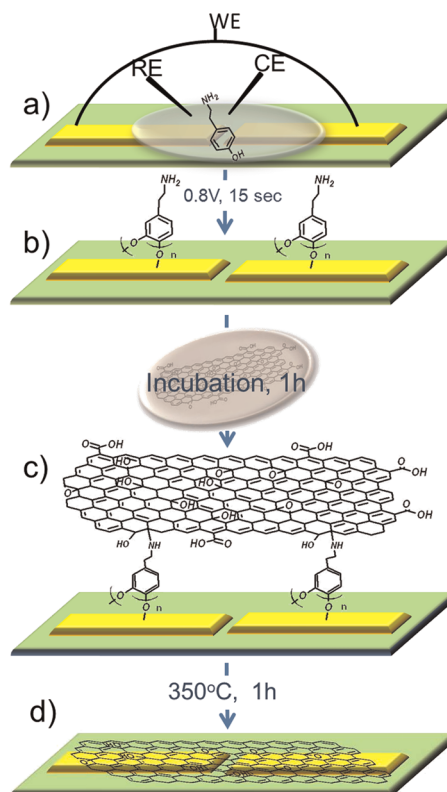

Figure 1. Scheme of the chemical anchoring protocol: (a) electrochemical functionalization of Pt electrodes with tyramine leading to (b) a coating of polytyramine on the electrode surface; (c) incubation of the chip in a GO solution results in the coupling of GO flakes to the polytyramine layer; (d) annealing in argon at 350 °C leads to the removal of the polytyramine layer and the reduction of most of the oxygen-containing groups. WE = working electrode, CE = counter electrode, RE = reference electrode.

various stages. It is apparent from the AFM image that the GO flake is comfortably positioned at the gap between the electrodes. Large-area images of the substrates confirm that GO is attached exclusively to the modified electrodes (see Supporting Information). On substrates not treated with tyramine no GO flakes were observed. The line profiles (Figure 2b) show the height of the bare electrode region (without GO) at the various stages: initial, after electrodeposition of polytyramine, and after the final annealing step. From the height profiles it is apparent that the layer of polytyramine that is formed on the surface of the electrodes during electrochemical functionalization has a thickness of around 5–8 nm. After thermal annealing, the height of the electrodes decreases to the initial value, indicating the removal of the polymer layer from the surface of the electrodes. Similar height profile analysis of the electrode regions with GO on top suggests the removal of the polymer layer also below the GO sheet (see Supporting Information).

The electronic properties of the realized RGO devices were investigated in parallel. Toward this goal, the resistance of the devices was measured with the help of impedance spectroscopy at various stages.
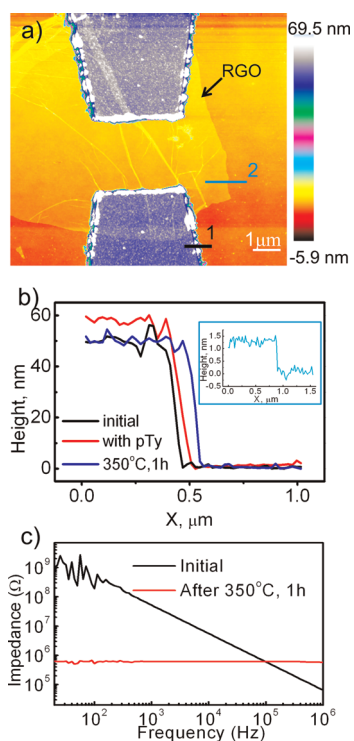
Figure 2. Characterization of the devices by AFM and electrical measurements. (a) AFM image of a typical sample obtained at the end of the chemical anchoring protocol. The electrode gap and the immobilized graphene oxide flake are visible here. (b) Height profiles (along the black line (1) in the AFM image taken at a GO-free region on the electrode, as extracted from AFM images recorded at various stages of the anchoring procedure. It is apparent that the pTy film after electrodeposition is 5 to 8 nm thick (red curve). Annealing leads to the reduction in electrode height (blue curve) to the initial value, signifying the removal of the pTy film. (Inset) Height profile of RGO taken along the blue line (2) on the AFM image. (c) Impedance spectrum of a typical anchored GO device before and after the thermal annealing step (350 °C, argon, 1 h), ac amplitude 100 mV. Before annealing the device is capacitive, signifying a high resistance in the GOhm range. Upon annealing the resistance has decreased to 600 kOhm. It can be inferred that the annealing step significantly reduces the resistance of the anchored flake.

Figure 2c shows the impedance of a typical device before and after the final annealing step. It is apparent that the RGO flake is insulating initially, as inferred from the capacitive behavior of the impedance spectrum.[29] After thermal annealing, the resistance improves to less than a MOhm and is stable in a broad frequency range. A similar behavior was observed in other samples with resistances in the range 200 kOhm to 2 MOhm. This resistance improvement confirms the removal of a majority of oxygen functionalities from the GO surface.[30] In order to gather further support for the improvement in electrical transport, the devices were investigated using Kelvin probe force microscopy (see Supporting Information).[31−33]

The advantage of this approach for device fabrication is the possibility to scale-up the process. Toward this goal, we utilized a specialized layout as shown in Figure 3a. The substrates were composed of 6 mm × 30 mm Si/SiO$_2$ chips, allowing for long leads. The long leads enable us to perform electronic transport measurements in liquids, as is discussed later. Each chip has six electrode gaps. All 12 electrodes are initially wire-bonded in the outer region of the substrate to form a parallel connection of 12 electrodes. In this manner all the electrodes can be decorated electrochemically with polytyramine in a single step. After the functionalization, the wire bonds are removed to obtain six individual devices. The remaining steps were carried out in the same manner as described before. Finally, in order to allow the use of such devices in liquids, the electrode surfaces were passivated with SiO$_2$.[29,34] Passivation of the metal electrodes with an insulating layer is a crucial step for some applications, such as sensing of biomolecules in liquids.[34,35] Since the positions of the electrodes are known beforehand, the passivation step can be carried out using a second photo mask with the help of alignment marks. Figure 3b presents AFM images of the six resulting passivated RGO devices from one chip. It is apparent that by performing all the necessary steps only once we have obtained a yield of six devices. In order to demonstrate the versatility of such devices for sensing applications, the field-effect behavior of the fabricated devices was investigated in liquids. For this purpose, a microwell made of polydimethylsiloxane is realized to hold the liquid on the substrates as shown in Figure 3a.[34] An Ag/AgCl electrode immersed in the liquid is used as the reference electrode. The gate dependence of resistance of one of the devices is shown in Figure 3c, which is reminiscent of the typical gate characteristics observed in the other back-gated and electrochemically gated RGO devices.[36−39] The gate dependence is ambipolar and has a broad peak corresponding to the Dirac point. The observed Dirac voltage (50−100 mV) is different from the previously reported value (200 mV). This difference may arise due to the use of a different reference electrode and/or due to a difference in the materials used for contacting and passivation. Variability in the number of graphene layers, in buffer composition, and in the extent of graphene oxide reduction may also contribute to this shift.

Due to the high sensitivity to chemical changes in their surroundings, nanomaterials show great promise for application as transducer components of various chemical and biological sensors.[40] Carbon nanotubes and graphene have been used widely for fabrication of electrical sensors for detection of sugars, nucleic acids, gas molecules, proteins, etc.[2,6,31,42−46] To demonstrate the potential of presented self-assembled RGO devices as biosensors, the detection of amyloid beta peptide was carried out, due to its importance in Alzheimer's disease.[23] In order to be able to detect amyloid beta with a high specificity, anti-Aβ-antibody was used as a
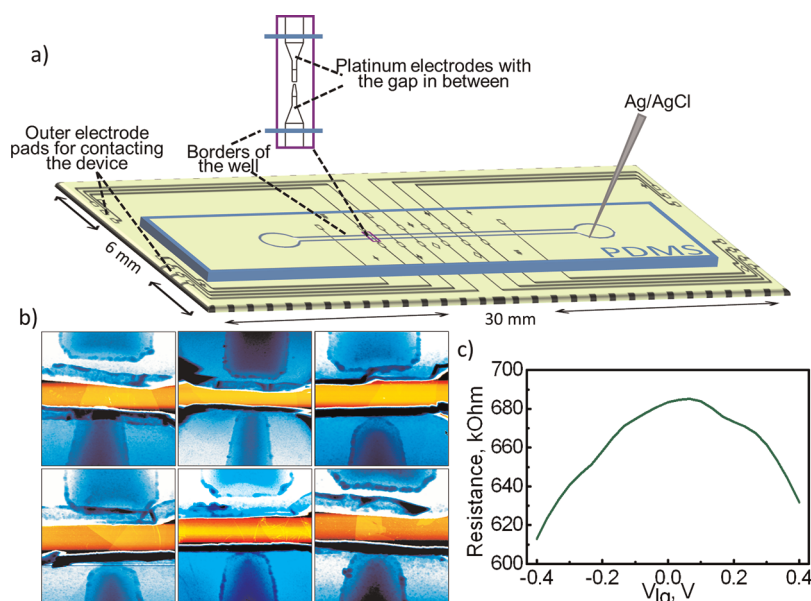
Figure 3. Scaling-up chemical anchoring. (a) Device layout showing six electrode gaps. Initially, the 12 electrodes are linked externally through wire bonding. For liquid-gating measurements, a liquid channel connected by two circular wells is created with the help of a polydimethylsiloxane layer. The inset shows a close-up of the electrode gap and the relative extent of the liquid channel. An Ag/AgCl reference electrode inserted in the channel serves as the gate electrode. **(b)** AFM images of the six gap positions (from one chip) at the end of the chemical anchoring protocol. In addition to the steps shown in Figure 1, the electrodes are passivated with SiO_2 using a separate photo mask. **(c)** Liquid gate dependence of resistance of one of the RGO devices, showing the typical ambipolar behavior.

receptor and was immobilized on the RGO surface in a two-step procedure. In a first step, RGO was covered with *Staphylococcus aureus* protein A (SpA) through carbodiimide coupling.[47] SpA ensures a proper orientation of the subsequently immobilized antibodies since it has high specificity to the *Fc* fragments.[48] It is expected that SpA attaches covalently to the carboxyl groups remaining in RGO. In a second step, SpA-RGO was modified with anti-Aβ-antibodies by incubating the samples in a 50 mM antibody solution. Finally, the samples were thoroughly washed with the buffer before the sensing trials. Figure 4b presents the field-effect characteristics of a typical RGO immunosensor device at the various stages of fabrication along with the response to amyloid beta peptide. Figure 4c shows the sensor response of another control sample to Aβ without using any antibodies. It is apparent that while the immunosensor shows a clear response to 1 fM Aβ, the control sample does not show changes in transport characteristics upon introduction of 1 fM and 100 pM amyloid beta solutions. This demonstration serves as a proof-of-principle for the use of our self-assembled RGO sensors as sensitive and selective electrical biodetectors. It is worth pointing out that the sensitivity of this device is about 1 order of magnitude higher than commercially available ELISA assays for Aβ quantification in biological fluids.[49]

From the foregoing discussions it is apparent that the chemical anchoring protocol serves as a versatile route to obtain RGO field-effect devices with a high throughput at the location of interest. The real
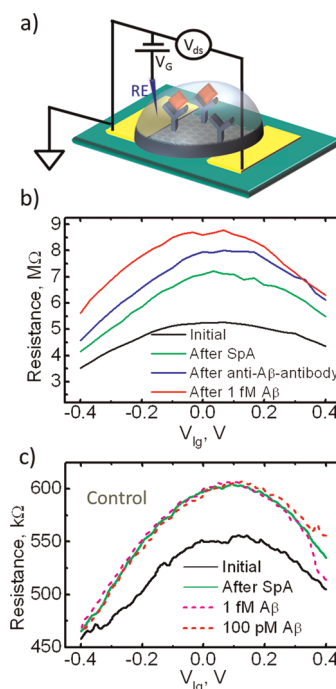

Figure 4. Sensing of amyloid beta peptide using RGO immunosensor. (a) Schematic of RGO-FET immunosensor; RE = reference electrode. **(b)** Field-effect characteristics of the RGO immunosensor before and after functionalization and after the exposure of antibody-functionalized device to 1 fM Aβ. **(c)** Control device showing the field-effect characteristics of another RGO device without the antibody.

advantage of such a technique in an industrial scenario requires the demonstration of such a protocol at the wafer scale. Furthermore, it will be important to
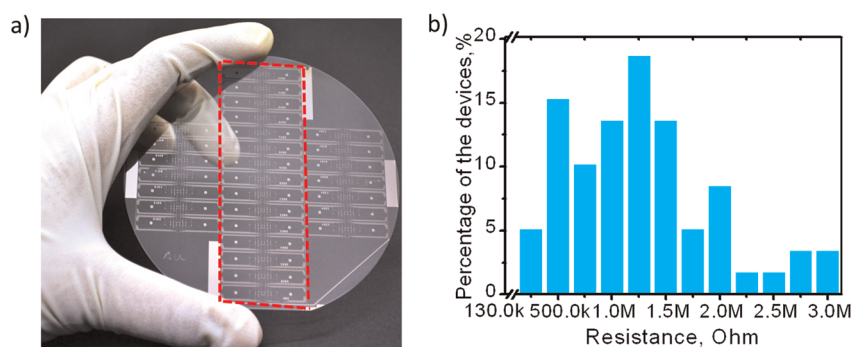
Figure 5. Wafer-scale RGO devices with high yield. (a) Photograph of a 4 in. glass wafer with photolithographically patterned electrodes. The electrodes in the red dashed region are connected to each other through the large pads in the upper left and lower bottom. These large pads are used to deposit a polytyramine layer on all the electrodes in a single step. There are 15 chips in the red dashed region, each chip containing six electrode gaps with an electrode layout as shown in Figure 3a. **(b)** Histogram of resistances of 77 out of the 90 electrode gaps at the end of the chemical anchoring protocol. Thirteen devices showed very high resistances (more than 3 MOhm).

evaluate the feasibility of this protocol on other substrates such as glass or polymers. With these aims in mind, we have fabricated electrodes on 4 in. glass wafers using photolithography as shown in Figure 5a. The wafer is segmented into chips, each of which is laid out as shown in Figure 3a. The layout is designed in such a way that the electrodes of the chips in the region marked with the red dashed line are all connected to each other through the large common pads. After carrying out the chemical anchoring protocol, the wafer is diced whereby these electrode connections are lost, resulting in stand-alone chips with six individual gaps each. For the wafer shown in Figure 5a, 77 working devices (out of 90 electrode gaps) were obtained, signifying a yield of 86%. A histogram of the resistances from these 77 devices is presented in Figure 5b, with resistances in the range 200 kOhm to 3 MOhm. These results underline the scalability of this approach, demonstrating the capability to obtain RGO devices at a high yield. The devices prepared on wafers showed higher resistances on average in comparison to those observed on individual samples. This could be improved by optimizing the conditions of electropolymerization and thermal reduction for the substrate of interest. It is worth mentioning here that this approach was also successfully implemented on substrates with differing electrode geometries, as well as on flexible

Kapton foils. Commercially available graphene oxide could also be coupled using this procedure (see Supporting Information).

CONCLUSIONS

In conclusion, we have demonstrated a new approach for the large-scale fabrication of RGO devices, which can subsequently be deployed as sensitive electrical biosensors. It allows preparing arrays of RGO devices in a short time without the use of serial techniques such as electron beam lithography. The chemical anchoring protocol involves the rendering of prepatterned electrode surfaces with amine groups. With the help of oxygen-containing moieties on the GO surface, the flakes are coupled to the amino groups by cross-linking. Using a thermal annealing step, the contacts could be improved and the oxygen functionalities removed to a large extent. A field-effect was observed on these devices when operating in liquids in an electrochemical gating configuration. The ability to realize wafer-scale RGO devices on arbitrary substrates is an important step toward their widespread use in a number of applications. As a proof-of-principle, we successfully demonstrated the sensitive immunodetection of amyloid beta peptides in buffer. Future experiments will focus on the deployment of such sensors in realistic biological media such as serum.

EXPERIMENTAL SECTION

The polymerization of tyramine was carried out by applying 0.8 V (*versus* Pt) for 15 s to the platinum electrodes on the Si/SiO$_2$ substrates immersed in a 10 mM tyramine solution with 10 mM H$_2$SO$_4$ using a CompactStat potentiostat (Ivium Technologies). Platinum wires were used as counter and pseudoreference electrodes. After electrochemical deposition of polytyramine the substrate was washed with ethanol and water and dried in nitrogen flow. An aqueous solution of graphene oxide was prepared using graphite powder by the Hummers method.[19,50] For the coupling of pTy with graphene oxide, we immersed the

substrate in the suspension of graphene oxide and left it for 1 h in a shaker. After the substrate was taken out of the GO solution it was immediately thoroughly washed with water and 2-propanol and dried in nitrogen flow. Following this, thermal annealing was carried out in an inert atmosphere (argon) at 350 °C for 1 h. After cooling to room temperature the sample was washed with 2-propanol and dried. Impedance measurements were carried out using an Agilent E4980A LCR meter. AFM images and surface potential maps were obtained using a Veeco/Digital Instruments Dimension IV.

The procedure for the functionalization of RGO with the antibody is described in the Supporting Information. For the sensing experiments impedance spectra (20 Hz to 2 MHz) of the devices were recorded in 10 mM phosphate buffer (pH 7.4) containing 100 mM NaCl at different gate voltages provided by an Ag/AgCl reference electrode.[34]

Conflict of Interest: The authors declare no competing financial interest.

Supporting Information Available: Protocols for the preparation of graphene oxide, biochemical functionalization of reduced graphene oxide, and the preparation of amyloid beta dispersions; large-area optical microscope images of RGO devices, additional AFM images and height profiles of (reduced) graphene oxide; comparison of the presented approach for device fabrication with dielectrophoretic trapping. This material is available free of charge *via* the Internet at http://pubs.acs.org.

REFERENCES AND NOTES

1. Brownson, D. A.; Banks, C. E. Graphene Electrochemistry: an Overview of Potential Applications. *Analyst* **2010**, *135*, 2768–2778.
2. Chen, F.; Qing, Q.; Xia, J.; Tao, N. Graphene Field-Effect Transistors: Electrochemical Gating, Interfacial Capacitance, and Biosensing Applications. *Chem. Asian J.* **2010**, *5*, 2144–2153.
3. Wang, Y.; Li, Z.; Wang, J.; Li, J.; Lin, Y. Graphene and Graphene Oxide: Biofunctionalization and Applications in Biotechnology. *Trends Biotechnol.* **2011**, *29*, 205–212.
4. Sakhaee-Pour, A.; Ahmadian, M. T.; Vafai, A. Applications of Single-Layered Graphene Sheets as Mass Sensors and Atomistic Dust Detectors. *Solid State Commun.* **2008**, *145*, 168–172.
5. Stoller, M. D.; Park, S.; Zhu, Y.; An, J.; Ruoff, R. S. Graphene-Based Ultracapacitors. *Nano Lett.* **2008**, *8*, 3498–3502.
6. Sundaram, R. S.; Gomez-Navarro, C.; Balasubramanian, K.; Burghard, M.; Kern, K. Electrochemical Modification of Graphene. *Adv. Mater.* **2008**, *20*, 3050–3053.
7. Choi, S. H.; Kim, Y. L.; Byun, K. M. Graphene-on-Silver Substrates for Sensitive Surface Plasmon Resonance Imaging Biosensors. *Opt. Express.* **2011**, *19*, 458–466.
8. Novoselov, K. S.; Geim, A. K.; Morozov, S. V.; Jiang, D.; Zhang, Y.; Dubonos, S. V.; Grigorieva, I. V.; Firsov, A. A. Electric Field Effect in Atomically Thin Carbon Films. *Science* **2004**, *306*, 666–669.
9. Liu, Z.; Bol, A. A.; Haensch, W. Large-Scale Graphene Transistors with Enhanced Performance and Reliability Based on Interface Engineering by Phenylsilane Self-Assembled Monolayers. *Nano Lett.* **2010**, *11*, 523–528.
10. Kim, K. S.; Zhao, Y.; Jang, H.; Lee, S. Y.; Kim, J. M.; Kim, K. S.; Ahn, J.-H.; Kim, P.; Choi, J.-Y.; Hong, B. H. Large-Scale Pattern Growth of Graphene Films for Stretchable Transparent Electrodes. *Nature* **2009**, *457*, 706–710.
11. Li, X.; Cai, W.; An, J.; Kim, S.; Nah, J.; Yang, D.; Piner, R.; Velamakanni, A.; Jung, I.; Tutuc, E.; *et al.* Large-Area Synthesis of High-Quality and Uniform Graphene Films on Copper Foils. *Science* **2009**, *324*, 1312–1314.
12. Hernandez, Y.; Nicolosi, V.; Lotya, M.; Blighe, F. M.; Sun, Z.; De, S.; McGovern, I. T.; Holland, B.; Byrne, M.; Gun'Ko, Y. K.; *et al.* High-Yield Production of Graphene by Liquid-Phase Exfoliation of Graphite. *Nat. Nano* **2008**, *3*, 563–568.
13. Tang, Z.; Zhuang, J.; Wang, X. Exfoliation of Graphene from Graphite and Their Self-Assembly at the Oil−Water Interface. *Langmuir* **2010**, *26*, 9045–9049.
14. Lotya, M.; Hernandez, Y.; King, P. J.; Smith, R. J.; Nicolosi, V.; Karlsson, L. S.; Blighe, F. M.; De, S.; Wang, Z.; McGovern, I. T.; *et al.* Liquid Phase Production of Graphene by Exfoliation of Graphite in Surfactant/Water Solutions. *J. Am. Chem. Soc.* **2009**, *131*, 3611–20.
15. Khan, U.; O'Neill, A.; Lotya, M.; De, S.; Coleman, J. N. High-Concentration Solvent Exfoliation of Graphene. *Small* **2010**, *6*, 864–871.
16. Smith, R. J.; Lotya, M.; Coleman, J. N. The Importance of Repulsive Potential Barriers for the Dispersion of Graphene Using Surfactants. *New J. Phys.* **2010**, *12*, 125008.
17. Stankovich, S.; Dikin, D. A.; Piner, R. D.; Kohlhaas, K. A.; Kleinhammes, A.; Jia, Y.; Wu, Y.; Nguyen, S. B. T.; Ruoff, R. S. Synthesis of Graphene-Based Nanosheets via Chemical Reduction of Exfoliated Graphite Oxide. *Carbon* **2007**, *45*, 1558–1565.
18. Dreyer, D. R.; Park, S.; Bielawski, C. W.; Ruoff, R. S. The Chemistry of Graphene Oxide. *Chem. Soc. Rev* **2010**, *39*, 228–240.
19. Gómez-Navarro, C.; Weitz, R. T.; Bittner, A. M.; Scolari, M.; Mews, A.; Burghard, M.; Kern, K. Electronic Transport Properties of Individual Chemically Reduced Graphene Oxide Sheets. *Nano Lett.* **2007**, *7*, 3499.
20. Vijayaraghavan, A.; Sciascia, C.; Dehm, S.; Lombardo, A.; Bonetti, A.; Ferrari, A. C.; Krupke, R. Dielectrophoretic Assembly of High-Density Arrays of Individual Graphene Devices for Rapid Screening. *ACS Nano* **2009**, *3*, 1729–1734.
21. Joung, D.; Chunder, A.; Zhai, L.; Khondaker, S. I. High Yield Fabrication of Chemically Reduced Graphene Oxide Field Effect Transistors by Dielectrophoresis. *Nanotechnology* **2010**, *21*, 165202–6.
22. Burg, B. R.; Lütolf, F.; Schneider, J.; Schirmer, N. C.; Schwamb, T.; Poulikakos, D. High-Yield Dielectrophoretic Assembly of Two-Dimensional Graphene Nanostructures. *Appl. Phys. Lett.* **2009**, *94*, 053110.
23. Hardy, J.; Selkoe, D. J. The Amyloid Hypothesis of Alzheimer's Disease: Progress and Problems on the Road to Therapeutics. *Science* **2002**, *297*, 353–356.
24. Losic, D.; Cole, M.; Thissen, H.; Voelcker, N. H. Ultrathin Polytyramine Films by Electropolymerisation on Highly Doped p-Type Silicon Electrodes. *Surf. Sci.* **2005**, *584*, 245–247.
25. Stern, E.; Jay, S.; Bertram, J.; Boese, B.; Kretzschmar, I.; Turner-Evans, D.; Dietz, C.; LaVan, D. A.; Malinski, T.; Fahmy, T.; Reed, M. A. Electropolymerization on Microelectrodes: Functionalization Technique for Selective Protein and DNA Conjugation. *Anal. Chem.* **2006**, *78*, 6340–6346.
26. Park, S.; Dikin, D. A.; Nguyen, S. T.; Ruoff., R. S. Graphene Oxide Sheets Chemically Cross-Linked by Polyallylamine. *J. Phys. Chem. C* **2009**, *113*, 15801–15804.
27. Tran, L. D.; Piro, B.; Pham, M. C.; Ledoan, T; Angiari, C.; Dao, L. H.; Teston, F. A Polytyramine Film for Covalent Immobilization of Oligonucleotides and Hybridization. *Synth. Met.* **2003**, *139*, 251–262.
28. Liu, M.-Q.; Jiang, J.-H.; Feng, Y.-L.; Shen, G.-L.; Yu, R.-Q. Glucose Biosensor Based on Immobilization of Glucose Oxidase in Electrochemically Polymerized Polytyramine Film and Overoxidised Polypyrrole Film on Platinized Carbon Paste Electrode. *Chin. J. Anal. Chem.* **2007**, *35*, 1435–1438.
29. Vlandas, A.; Kurkina, T.; Ahmad, A.; Kern, K.; Balasubramanian, K. Enzyme-Free Sugar Sensing in Microfluidic Channels with an Affinity-Based Single-Wall Carbon Nanotube Sensor. *Anal. Chem.* **2010**, *82*, 6090–6097.
30. Kang, H.; Kulkarni, A.; Stankovich, S.; Ruoff, R. S.; Baik, S. Restoring Electrical Conductivity of Dielectrophoretically Assembled Graphite Oxide Sheets by Thermal and Chemical Reduction Techniques. *Carbon* **2009**, *47*, 1520–1525.
31. Melitz, W.; Shen, J.; Kummel, A. C.; Lee, S. Kelvin Probe Force Microscopy and Its Application. *Surf. Sci. Rep.* **2011**, *66*, 1–27.
32. Nonnenmacher, M.; O'Boyle, M. P.; Wickramasinghe, H. K. Kelvin Probe Force Microscopy. *Appl. Phys. Lett.* **1991**, *58*, 2921–2923.
33. Yan, L.; Punckt, C.; Aksay, I. A.; Mertin, W.; Bacher, G. Local Voltage Drop in a Single Functionalized Graphene Sheet Characterized by Kelvin Probe Force Microscopy. *Nano Lett.* **2011**, *11*, 3543–354.

34. Kurkina, T.; Vlandas, A.; Ahmad, A.; Kern, K.; Balasubramanian, K. Label-Free Detection of Few Copies of DNA with Carbon Nanotube Impedance Biosensors. *Angew. Chem., Int. Ed.* **2011**, *50*, 3710–3714.

35. Balasubramanian, K. Challenges in the Use of 1D Nanostructures for On-Chip Biosensing and Diagnostics. *Biosens. Bioelectron.* **2010**, *26*, 1195–1204.

36. Jung, I.; Dikin, D. A.; Piner, R. D.; Ruoff, R. S. Tunable Electrical Conductivity of Individual Graphene Oxide Sheets Reduced at "Low" Temperatures. *Nano Lett.* **2008**, *8*, 4283–4287.

37. He, Q.; Wu, S.; Gao, S.; Cao, X; Yin, Z.; Li, H.; Chen, P.; Zhang, H. Transparent, Flexible, All-Reduced Graphene Oxide Thin Film Transistors. *ACS Nano* **2011**, *5*, 5038–5044.

38. Yin, Z.; He, Q.; Huang, X.; Zhang, J.; Wu, S.; Chen, P.; Lu, G.; Chen, P.; Zhang, Q.; Yan, Q.; Zhang, H. Real-Time DNA Detection using Pt Nanoparticle-Decorated Reduced Graphene Oxide Field-Effect Transistors. *Nanoscale* **2012**, *4*, 293–297.

39. Sudibya, H. G.; He, Q.; Zhang, H.; Chen, P. Electrical Detection of Metal Ions Using Field-Effect Transistors Based on Micropatterned Reduced Graphene Oxide Films. *ACS Nano* **2011**, *5*, 1990–1994.

40. Kurkina, T. Kannan Balasubramanian. Towards *in vitro* Molecular Diagnostics Using Nanostructures. *Cel. Mol. Life Sci.* **2012**, *69*, 373–388.

41. Mao, S.; Lu, G.; Yu, K.; Bo, Z.; Chen, J. Specific Protein Detection Using Thermally Reduced Graphene Oxide Sheet Decorated with Gold Nanoparticle-Antibody Conjugates. *Adv. Mater.* **2010**, *22*, 3521–3526.

42. Lu, G.; Park, S.; Yu, K.; Ruoff, R. S.; Ocola, L. E.; Rosenmann, D.; Chen, J. Toward Practical Gas Sensing with Highly Reduced Graphene Oxide: a New Signal Processing Method to Circumvent Run-to-Run and Device-to-Device Variations. *ACS Nano* **2011**, *5*, 1154–1164.

43. Dua, V.; Surwade, S. P.; Ammu, S.; Agnihotra, S. R.; Jain, S; Roberts, K. E.; Park, S.; Ruoff, R. S.; Manohar, S. K. All-Organic Vapor Sensor Using Inkjet-Printed Reduced Graphene Oxide. *Angew. Chem., Int. Ed.* **2010**, *49*, 2154–2157.

44. Robinson, J. T.; Perkins, F. K.; Snow, E. S.; Wei, J.; Sheehan, P. E. Reduced Graphene Oxide Molecular Sensors. *Nano Lett.* **2008**, *8*, 3137–3140.

45. Balasubramanian, K.; Burghard, M. Biosensors Based on Carbon Nanotubes. *Anal. Bioanal. Chem.* **2006**, *385*, 452–462.

46. Yang, W.; Ratinac, K. R.; Ringer, S. P.; Thordarson, P.; Gooding, J. J.; Braet, F. Carbon Nanomaterials in Biosensors: Should You Use Nanotubes or Graphene? *Angew. Chem., Int. Ed.* **2010**, *49*, 2114–2138.

47. Johnsson, B.; Löfås, S.; Lindquist, G. Immobilization of Proteins to a Carboxymethyldextran-Modified Gold Surface for Biospecific Interaction Analysis in Surface Plasmon Resonance Sensors. *Anal. Biochem.* **1991**, *198*, 268–277.

48. Turková, J. Oriented Immobilization of Biologically Active Proteins as a Tool for Revealing Protein Interactions and Function. *J. Chromatogr., B: Anal. Technol. Biomed. Life Sci.* **1999**, *722*, 11–31.

49. Cazzaniga, E.; Bulbarelli, A.; Lonati, E.; Orlando, A.; Re, F.; Gregori, M.; Masserini, M. Abeta Peptide Toxicity is Reduced after Treatments Decreasing Phosphatidylethanolamine Content in Differentiated Neuroblastoma Cells. *Neurochem. Res.* **2011**, *36*, 863–869.

50. Hummers, W. S.; Offeman, R. E. Preparation of Graphitic Oxide. *J. Am. Chem. Soc.* **1958**, *80*, 1339–1339.